October 1996 • NREL/TP-451-21718

Optimization of Laser Scribing for Thin-Film PV Modules

Annual Technical Progress Report 12 April 1995 - 11 April 1996

A.D. Compaan, U. Jayamaha,
I. Matulionis, and M.J. Miller
University of Toledo
Toledo, Ohio

National Renewable Energy Laboratory
1617 Cole Boulevard
Golden, Colorado 80401-3393
A national laboratory of
the U.S. Department of Energy
Managed by Midwest Research Institute
for the U.S. Department of Energy
under Contract No. DE-AC36-83CH10093

Summary

This report covers the first year of a two-year project to investigate the use of four different types of lasers for scribing of materials used for polycrystalline thin-film photovoltaics. The materials under investigation include semiconductors (cadmium telluride and copper indium gallium diselenide), transparent conducting oxides (fluorine-doped tin oxide and aluminum-doped zinc oxide), and a metal (molybdenum). The laser systems are all commercially available and were chosen for the range of pulse durations and wavelengths available. We used a continuous krypton-lamp-pumped, Q-switched Nd:YAG laser with a wavelength of λ=532 nm, a flashlamp-pumped-Nd:YAG laser (λ=532 or 1064 nm), a copper-vapor laser (λ=511 and 578 nm), and an XeCl-excimer laser (λ=308 nm). In addition to the different wavelengths, these systems were chosen for the range of pulse durations available. The pulse durations range from 100- 600 nsec for the cw/Q-switched YAG, 55 nsec for the Cu-vapor, 20 nsec for the excimer, to 10 nsec for the flashlamp-pumped, Q-switched YAG. The laser systems and beam focussing options are being evaluated from the point of view of the efficiency of pulse energy utilization, potential for high scribing velocity, and scribe quality (e.g., electrical isolation, narrow scribe width, small heat-affected zone, and minimum ejecta rim at the scribe edge).

Table of Contents

List of Figures

List of Tables

Introduction and Objectives

One of the most important aspects in moving from the cell level to the integrated module level in thin-film photovoltaics is to achieve reliable and reproducible cell interconnects having low series resistance and high shunt resistance, and to do this with a minimum of dead area between cells. It is known that mechanical scribing often produces considerable damage (e.g., film tearing) surrounding the scribe. Laser scribing has shown the potential for superior scribe widths and profiles for many of the materials involved with thin-film PV. However, problems are also known to occur with a heat-affected zone around the scribe, and for some materials and some focus conditions high positive ridges or collars are left along the scribe line.

The commercially-available scribing systems have been optimized typically for other applications and other materials such as scribing of crystalline Si[1]. Optimum operation for thin-film PV materials has been investigated by several PV manufacturers[2,3,4] but there has been limited discussion of problems or of optimum parameters in the open literature. Furthermore, to our knowledge, there has been little investigation of the applicability, for thin-film PV, of laser systems other than the traditional cw lamp-pumped, Q-switched Nd:YAG[5,6].

This two-year project is designed to improve our fundamental understanding of the laser scribing process and the role of the variables of laser wavelength, laser pulse duration, and pulse energy density on the quality, speed, and efficiency of scribing of thin-film PV materials. The materials under investigation include the semiconductors cadmium telluride and copper indium gallium diselenide, the transparent conducting oxides, fluorine-doped tin oxide and aluminum-doped zinc oxide, and the metal, molybdenum. The laser systems are all commercial systems and were chosen for the range of pulse durations and wavelengths available. We used a continuous krypton-lamp-pumped and Q-switched Nd:YAG laser with a wavelength of λ=532 nm, a flashlamp-pumped-Nd:YAG laser (λ=532/1064 nm), a copper-vapor laser (511/578 nm), and an XeCl-excimer laser (308 nm). In addition to the different wavelengths, these systems were chosen for the range of pulse durations available. In the order listed above the lasers have pulse durations of 120-600 nsec, ~10 nsec, 55 nsec, and 20 nsec.

Laser Characteristics

The four lasers studied in this project have pulse durations ranging from 600 nsec to 8 nsec. The wavelengths range from 1064 nm to 308 nm. At the longest wavelength of 1064 nm, all of the thin-film PV materials studied except copper indium gallium diselenide (CIGS) are transparent or nearly transparent. At the shortest wavelength, all the thin-film materials studied here are strongly absorbing. In the following, we discuss the characteristics of each of the lasers individually, highlighting the differences among them. We want to emphasize here that these lasers do not necessarily represent state-of-the-manufacturers-art and in some cases the output specifications are well below those which are available today. For example, the flashlamp-pumped Nd:YAG system discussed below is a vintage ~1980 system and the 1988 manufacturer of our excimer laser is no longer in business. Nevertheless, the critical parameters of pulse duration and wavelength have not changed. Presently available systems typically have improved beam quality, stability and higher repetition rates. In Phase Two of the present contract, we intend to consider in more detail the commercially available laser systems and present recommendations for optimum methods of focussing, etc, which may depend on issues such as beam divergence, mode quality and pulse-to-pulse fluctuations.

The CW Kr-lamp-pumped, Q-switched Nd:YAG Laser

The first laser system described here is the most commonly used type of laser for commercial laser scribing systems. This continuous wave (CW) krypton-lamp-pumped and Q-switched Nd:YAG laser was a U. S. Laser model 403PQ adapted for use at SCI. We shall refer to this system as the "cw-pulsed" or CWP Nd:YAG system.

In the case of the CWP YAG laser, the pulse temporal profile is very smooth but does depend on the repetition frequency. This is a consequence of the fact that with the continuous pumping of the Nd:YAG rod by the Kr lamp, the degree of population inversion attained by the time the intracavity Q-switch opens is larger for the low repetition rates. Consequently the photon density in the resonator rises more quickly when the Q-switch opens and drives the population inversion quickly below threshold. (This behavior is observed even more clearly in the difference between the free-running mode and Q-switched mode in the flashlamp-pumped YAG laser, discussed in the next section. In that case, the non-Q-switched pulse duration could be as long at 400 nsec whereas the Q-switched pulse duration is about 10 nsec.) For the work reported here, the CWP Nd:YAG laser was operated at a pulse repetition frequency (PRF) of 5 kHz in the frequency doubled mode where the pulse duration was 180 nsec with a tail which extended to about 500 nsec after the pulse peak. See Fig. 1. We observed the pulse shape with a p-i-n photodiode and a Hewlett-Packard model 54510A 1Gsample/sec digitizing scope. The hard copy of the pulse shape was obtained via the HPIB interface to a personal computer. At 5 kHz the average power was about 2 W or 0.4 mJ/pulse in a single TEM_{00} mode.

SCI has provided us with their measurement of the relationship of the pulse duration to the repetition rate. This is shown in Fig. 2. Note that the pulse duration can range from 125 nsec at the lowest PRF (1 kHz) to 600 nsec at 30 kHz. This range of pulse durations can have important consequences on the morphology of the scribe for some PV materials. This system was operated at ~2W of average power at 5 kHz so that the pulse energy was 0.4 mJ.

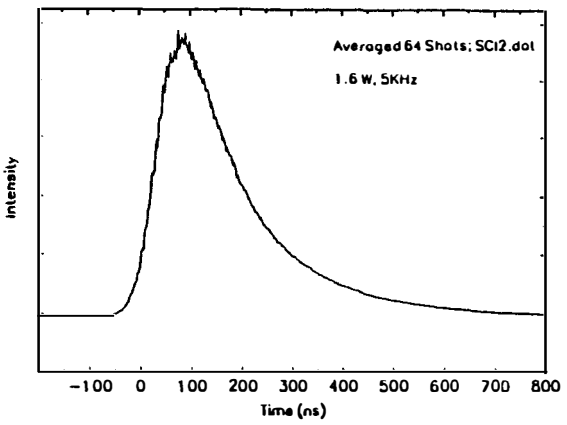

Fig. 1 Temporal pulse shape of CWP Nd:YAG laser at 5 kHz, λ = 532 nm.

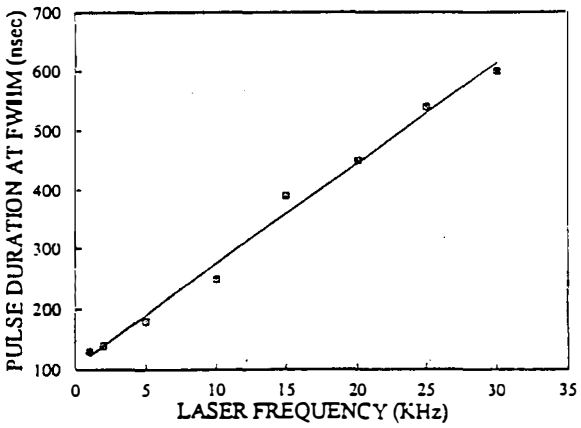

Fig. 2. Pulse duration vs. PRF for CWP Nd:YAG laser.

For this laser, the scribing was done with a 210 cm focal length lens. This lens yielded a spot size of about 75 μm. At the sample scan speed of 250 mm/sec, which we used for the initial study, the ablation spot spacing was 50 μm. This yielded nearly separated images of the ablation spots but with partial overlap so that the maximum ablation depth usually occurred at the overlap region of adjacent pulses rather than at the center of each pulse. See Fig. 12 and the discussison under Scribe Quality.

The Flashlamp-pumped Nd:YAG Laser

Commercial laser scribing systems generally utilize the CWP Nd:YAG laser engine, discussed above, which typically have minimum output pulse durations of about 100 nsec. (See Fig. 2 above.) In order to explore the effects of shorter pulse durations with the same wavelengths, we used a flashlamp-pumped, Q-switched Nd:YAG laser. We shall refer to this as the FLP YAG. This is a Quanta-Ray DCR-1A oscillator/amplifier system at the University of Toledo. This laser may be operated either in the "free running" mode without activating the Q-switch, or in the Q-switched mode. This system, even without the use of the amplifier stage, has very high pulse energy, typically 100 mJ/pulse in the Q-switched mode at 1064 nm. Thus, in the present studies with spherical

focussing, we have used substantial attenuation of this beam. In addition the unstable resonator optics of this system do not give clean focal spot profiles without substantial aperturing. Nevertheless this laser, by virtue of its short pulse durations, provides an important comparison with the CWP YAG system.

Figure 3 shows that, when the laser is operated in the "free-running" mode, it emits trains of pulses (relaxation oscillations) with about half a dozen spikes near threshold to more than 50 at a flashlamp energy of 1.7 times threshold. These pulses are spread over a duration of about 50 μs near threshold to about 150 μs at the highest lamp energy. As shown in Fig. 4, the laser in this free running mode has individual pulse durations ranging from about 190 nsec to about 400 nsec depending on the flashlamp energy. The longest pulses occur at 33 J of lamp energy, very near the lasing threshold of 32 J. As the optical excitation increases and the gain increases, the pulse duration shortens considerably, down to typically 190 nsec. This behavior is very similar to the effect of repetition rate on the CWP Nd:YAG laser and again is a direct consequence of the degree of population inversion achieved when the lasing begins. The laser pulse duration is quite important in understanding how the optical energy is coupled into the film and this affects the optimum laser pulse energy and optimum focussing for scribing each material.

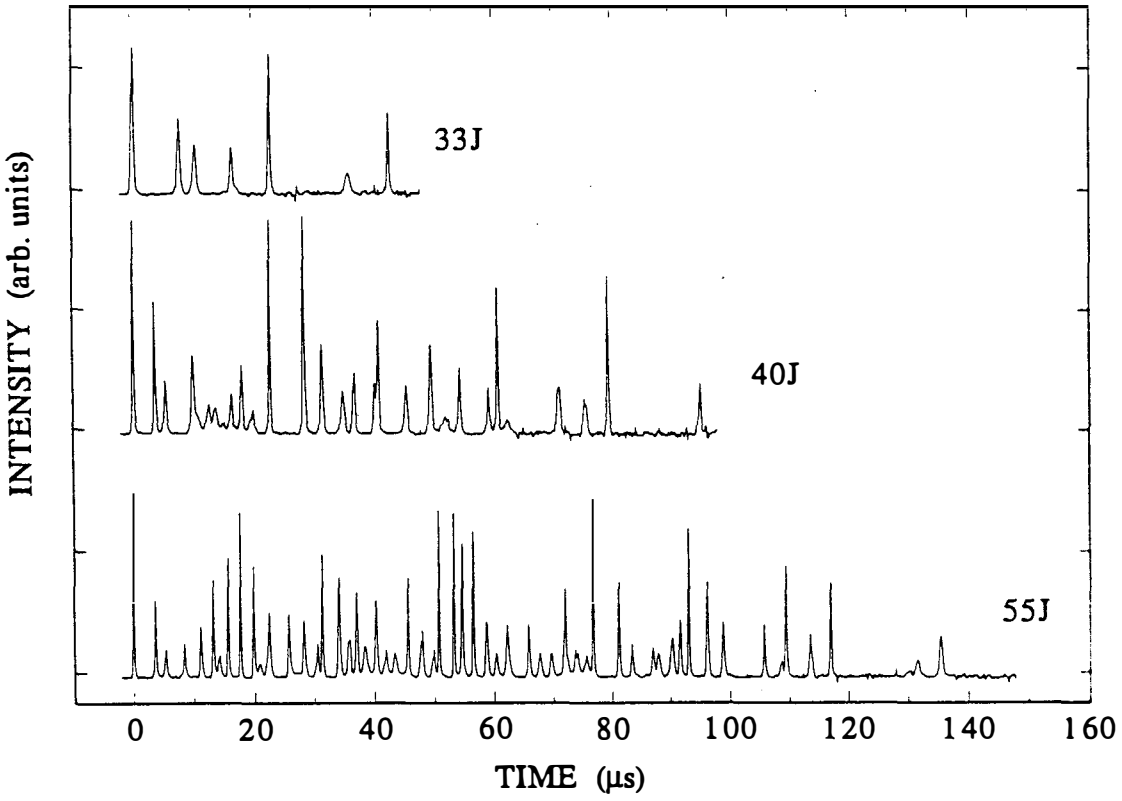

Fig. 3. Non-Q-switched output from FLP Nd:YAG laser showing spiking behavior for three different flashlamp energies. Note that time scales are different for each trace.

When Q-switching is used in the flashlamp-pumped Nd:YAG, lasing is held off as the Pockels cell spoils the gain (increases the resonator loss) in the laser cavity and much higher population inversion is produced in the laser rod until the resonator loss is rapidly switched low (on a time scale of 1 nsec--much less than the photon round trip time in the resonator). In this case the output pulse duration is very short, with the energy coupled out of the laser rod within 2 to 3 photon round trips in the resonator. The Q-switched pulsed durations of both the fundamental wavelength (1064 nm) and the frequency-doubled wavelength (532 nm) are shown in Figure 5. We find pulse durations of 11 nsec and 8 nsec, respectively, for the fundamental and frequency-doubled outputs. The

frequency-doubled pulse is slightly shorter in duration than the fundamental as a consequence of the nonlinear doubling process.

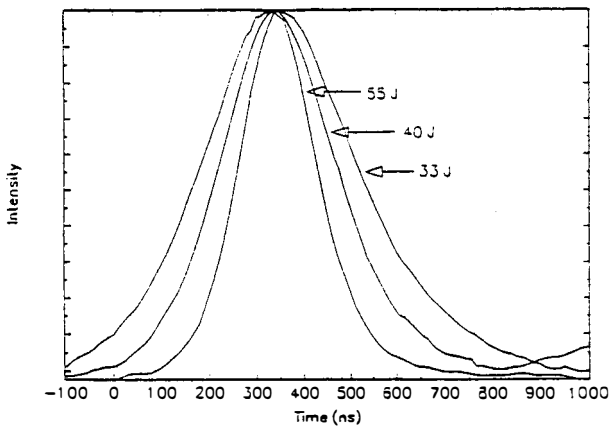

Fig. 4. Temporal pulse profiles of individual spikes of FLP Nd:YAG for three lamp energies.

The Copper-vapor Laser

The flashlamp-pumped Nd:YAG laser generates very short pulses and thus permits insight into the dependence on laser pulse duration. However, the repetition rate is limited by cooling of the flashlamps and the laser rod to about 100 Hz, typically (30 Hz for our system). The copper vapor laser allows access to shorter pulse durations (~50 nsec) while giving repetition rates similar to the CWP Nd:YAG.

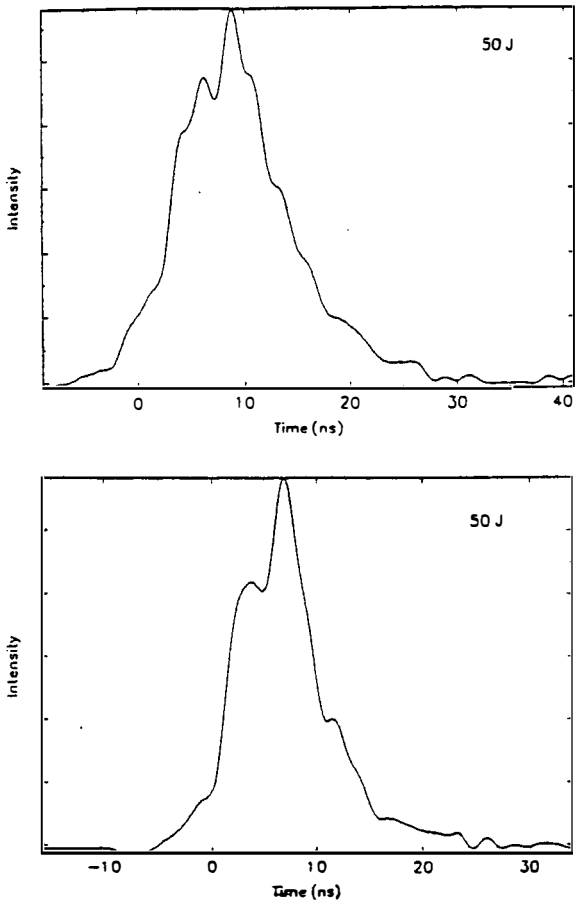

Fig. 5. Temporal pulse profile of Q-switched, FLP Nd:YAG. a) 1064 nm; b) 532 nm.

In order to study the performance of this laser for scribing applications, we brought a small x-y translation system to the applications lab of C J Laser in Dayton, OH. The copper-vapor laser (CJL model MVL-2210) has output transitions at 510.6 nm and 578 nm (green and yellow) with about 25 % of the 16 watts of power appearing in the yellow transition. Since the pulse repetition frequency was 8 kHz, the energy per pulse was 2 mJ. A plot of the pulse shape is given in Fig. 6. The full width at half maximum is 57 nsec. The pulse trace is very reproducible and shows some regular oscillation within the pulse envelope. These oscillations Probably arise from rf pick-up although there may be some contribution from the beating of longitudinal modes in this system with resonator length of 96 inches (246 cm). The Fabry-Perot resonances in a resonator of this length would yield a longitudinal mode spacing of $\Delta\nu = c/2L =$ 60 GHz. The beat period of adjacent longitudinal modes would be $T = 1/\Delta\nu =$ 16 nsec, very close to the observed oscillations. Note that there is essentially no tail of the lasing pulse beyond two half-widths from the pulse peak.

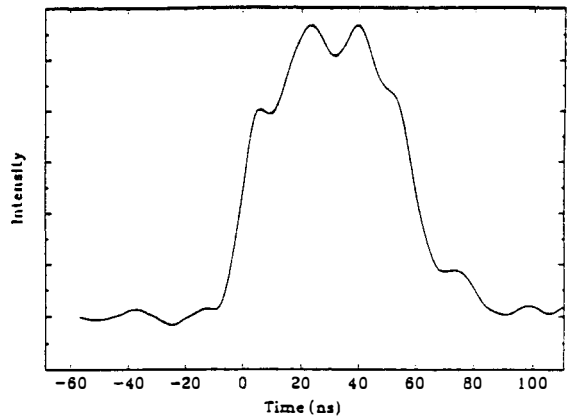

Fig. 6. Temporal profile of Cu-vapor laser pulse at 8 kHz.

The laser we used had an extended cavity design with unstable resonator optics. These optics provide a beam of about 20 mm diameter and a very low beam divergence of 0.1 mrad. Using a 100 mm focal length lens, we easily achieved scribe linewidths of 50 to 150 μm. One limitation of this system from our perspective in these early experiments is that the repetition rate of this laser system is not readily adjustable since the laser bore temperature is maintained by the longitudinal discharge itself. Our scanning system could achieve, at the time of our visit, a maximum translation speed of 13.5 mm/sec. Thus, for a 75 μm spot size each point on a scan line was addressed by approximately 45 overlapping pulses.

The XeCl Excimer Laser

There are several differences between the excimer laser and the other laser systems in this study. The transverse discharge XeCl laser has very high gain so that with standard plane-parallel mirrors (marginally stable resonator), the transverse mode quality is poor. In addition, the transverse discharge does not naturally produce an axially-symmetric beam. For our laser, a Questek model 2240 with a gas fill for XeCl, we typically run with a pulse energy of 80 mJ and repetition rates <30 Hz. Because of the high pulse energy and the poor beam quality of this laser we have typically used considerable aperturing of the beam and attenuation for convenience with the spherical focussing discussed here.

We observe a beam divergence in the horizontal and vertical directions of 10 mrad and 2 mrad respectively. Using a spherical lens the focal spot from our laser is approximately a rectangle and, with moderate aperturing, can produce a very fine line. In data presented below we provide results obtained with a spherical lens; however, we have preliminary data showing that the output beam profile can be utilized very conveniently, perhaps optimally, with a cylindrical focussing lens and translation along the long axis of the focal image. See Fig. 21 and related discussion. The short wavelength and short pulse duration, with resulting high peak power density, do not lend themselves to deep ablation with single shots. Rather multiple pulse ablation spots and lines most advantageously utilize the laser energy.

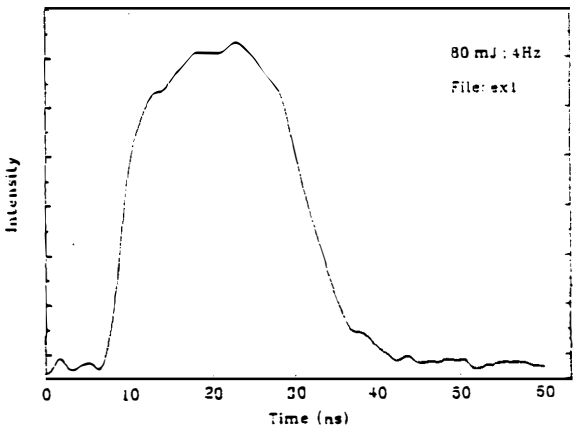

Fig. 7. Temporal profile of XeCl excimer laser pulse at 308 nm.

The temporal pulse profile of the excimer laser is shown in Fig. 7. The pulse profile exhibits a full width at half maximum of 20 nsec with a slight tail trailing to longer times. We are using He as the buffer gas in this laser which yields a slightly shorter pulse duration than Ne as a buffer gas but slightly lower pulse energies.

Laser Vaporization Thresholds

In the field of high power pulsed laser interaction with solids there has been a considerable discussion in the literature over the definition and interpretation of thermal evaporation vs. non-thermal "ablation"[7,8]. The distinctions center on whether the material removal is driven by heating of the near-surface region or by direct bond-breaking. We have chosen to use the term "vaporization" to avoid introducing loaded issues. In a first set of measurements we have determined the pulse energy density at the threshold for vaporization. For our definition of vaporization threshold, we used the operational condition of surface damage visible in an optical microscope.

A summary of the threshold energy densities for ablation is presented in Table 1[9]. Note that we are giving

thresholds in terms of the incident pulse energy with no correction for the reflected fraction. Thresholds are affected by the specific heat, the heat of fusion, and the heat of vaporization but the optical absorption length is the most important factor determining the ablation threshold in these thin-film materials. However, at longer pulse durations, thermal diffusion during the pulse also becomes a factor. The effect of pulse duration is clearly evident at 532 nm where the 180 nsec pulse gives a threshold two to three times higher than the 8 nsec pulse. Longer pulses allow for greater diffusion of heat into the film during the pulse, thus raising the threshold.

Wavelength-dependent effects are also clearly seen in Table 1. In the strongly absorbing semiconductors CdTe and $CuInGaSe_2$, the ablation thresholds are low as expected (similar to Ref. 10 for CIS and Moly), less than 0.5 J/cm^2 except for the case of CdTe at 1064 nm where the photon energy is below bandgap. The lowest thresholds for all materials are observed at 308 nm even though the excimer laser pulse duration is somewhat longer than the flashlamp-pumped YAG. These low thresholds arise from the very high absorption coefficients in the ultraviolet for all of these materials. Not surprisingly, the effects are particularly large for the transparent conducting oxides which are transparent at all the other wavelengths. Note that the ablation thresholds for SnO_2 and ZnO are only 10% or less of those observed in the green or infrared.

TABLE 1: Thresholds for Laser Scribing of Thin-film PV Materials

λ(nm)@Δτ	SnO_2 (J/cm^2)	CdTe (J/cm^2)	ZnO (J/cm^2)	CIGS (J/cm^2)	Mo (J/cm^2)
1064 @10ns	2.4	0.65	3.9	0.32	0.44
532 @10ns	4.5	0.10	3.5	0.15	0.30
532 @180ns	8*	0.3	13*	0.35	
308 @15ns	0.44	0.08	0.24	0.13	0.24
511, 578 @55ns	3.4	0.1	0.6	0.1	1.0

* large shot-to-shot variations

For the transparent oxide materials the pulse width dependence may arise from thermal diffusion effects but also may be affected by non-linear absorption effects since non-linear absorption will be stronger for the higher peak power, shorter duration pulses. For ZnO large spot-to-spot variations occur in the ablation threshold measurements presumably due to absorption processes which initiate at defects. In addition we find that the ablation threshold is much lower if the ZnO has been irradiated by previous laser pulses even if these have not produced visible damage -- again presumably caused by laser-irradiation-induced defect centers.

In the cases of the 1064 nm and 532 nm wavelengths with 10 ns pulses (FLP Nd:YAG) and the 308 nm excimer all threshold measurements were made with single pulses. However in the case of the 532 nm, 180 nsec pulses (CWP-Nd:YAG) the data were obtained from scans with two overlapping pulses. (See Fig. 12 below.) In the case of the copper-vapor laser (511 + 578 nm) the PRF was the highest (8 kHz) and the maximum scan rate was low (13.5 mm/sec) so that there were about 45 overlapping pulses. For these two cases, the numbers in Table 1 for the vaporization threshold should be treated with caution. For example the visual indication of surface damage may be affected by the temperature rise during the scan or by laser-induced defects. We expect to obtain new data on these systems in Phase Two without these limitations of overlapping pulses.

Optimum Energy Density for Scribing

Although the threshold energy for vaporization provides insight into the laser-solid interaction for each thin-film material, a more relevant issue for laser scribing of thin-film PV materials is to identify the conditions which will

provide the most efficient use of the laser energy and thus permit the fastest scribing of large-area panels. At threshold nearly all of the laser pulse energy is deposited as heat into the thin film and only a small fraction of the laser pulse energy goes into vaporization. But as the energy density rises a greater fraction of the pulse energy is useful in vaporization of materal. On the other hand, at least for the short pulse lasers, too much energy density results in increasing fractions of the trailing part of the laser pulse being absorbed in the vapor generated by the leading edge of the pulse. In this case, much of the laser pulse energy never reaches the film and the scribing efficiency is also low. Thus we expect to find an optimum energy density for scribing.

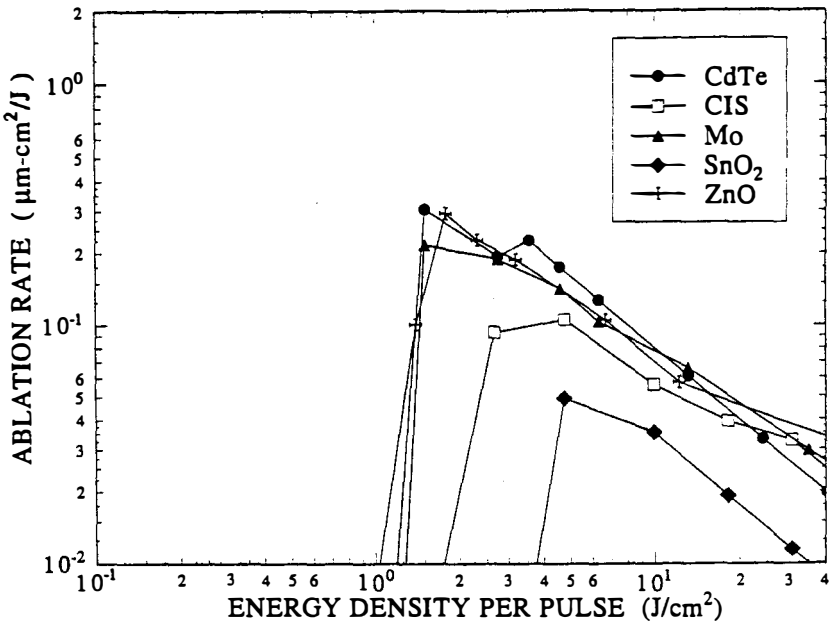

Fig. 8. Thickness vaporized in μm divided by energy density per pulse for 11 nsec pulse at 1064 nm.

We have determined the vaporized quantity per pulse by measuring the number of pulses required to fully vaporize films of known thickness. The films were typically 0.5 μm SnO_2, 2.0 μm CdTe, 2.0 μm CIGS, 2.5 μm moly, and 2.0 μm ZnO. Up to now the vaporization rate has been studied carefully only for the 10 nsec YAG and the excimer lasers. The CWP YAG system and the copper-vapor laser system will be studied early in Phase Two of this project.

Figure 8 shows the thickness vaporized per unit pulse energy density as a function of the energy density of the pulse for the 10 nsec YAG laser pulse at 1064 nm. The data were obtained by taking films of known thickness and determining the number of pulses needed to scribe through at each pulse energy density. For the visually opaque materials this was readily done in the optical microscope with rear illumination. For the composite structures such as CIS on Moly we relied on contrast or roughness changes and checked these with stylus profilometer measurements. For the transparent conducting oxides

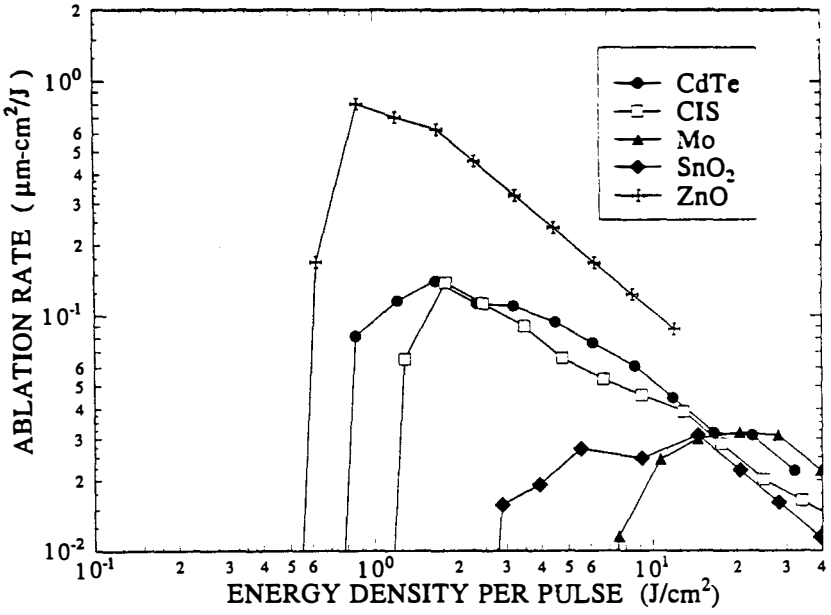

Fig. 9. Thickness vaporized in μm divided by energy density per pulse for 8 nsec pulse at 532 nm.

again there usually were visual differences at the glass/TCO interface which showed up in microscopic examinations. Results were checked with profilometer scans. Comparison with the thresholds given in Table 1 shows that the most efficient energy density for material vaporization occurs typically in the range of 3 to 10 times the ablation threshold.

Figures 9 and 10 show similar data for the 532 nm, 8 nsec frequency-doubled YAG and the 308 nm, 15 nsec XeCl excimer laser. Note that the general trends are similar to those reported recently in Ref. 10 for CdTe at 308 nm.

The maxima in the curves identify the energy densities which produce the largest amount of material vaporized per incident pulse energy density. This may also be expressed as the number of atoms vaporized per incident photon. Table 2 summarizes the results to date.

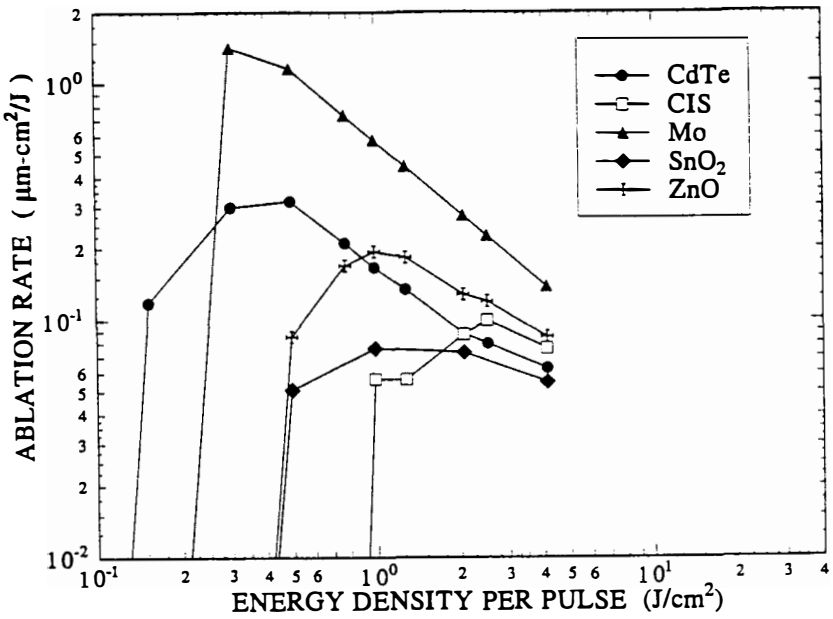

Fig. 10. Thickness vaporized in μm divided by energy density per pulse for 20 nsec excimer laser pulse at 308 nm.

TABLE 2: Optimum Efficiency for Laser Scribing of Thin-film PV Materials

λ(nm)@Δτ	SnO_2 (atoms/photon)	CdTe (atoms/photon)	ZnO (atoms/photon)	CIS (atoms/photon)	Mo (atoms/photon)
1064 @10ns	0.08 @ 5J/cm²	0.17 @1.7J/cm²	0.5 @1.7J/cm²	0.07 @ 4J/cm²	0.3 @ 1.7J/cm²
532 @10ns	0.01@14 J/cm²	0.15 @1.7J/cm²	2.5 @ 0.9J/cm²	0.17 @1.8J/cm²	0.01@ 20J/cm²
532 @180ns					
308 @15ns	0.4 @ 1.2 J/cm²	0.6 @0.35J/cm²	1.1 @ 1J/cm²	0.23 @2.5J/cm²	5.4 @ 0.4J/cm²
511, 578 @55ns					

Focussing Considerations

From the data of Table 2 we can infer conditions which will facilitate optimum utilization of the laser pulse energy. (Note that these conditions may not necessarily yield the optimum scribe quality! See below.) Thus for

the Cu-vapor laser operating with 16 W of power at 8 kHz PRF, the energy per pulse is 2 mJ. With a beam divergence of 0.1 milliradian, a 12.5 cm focal length lens will focus the beam to a 25 μm diameter spot and if we conservatively estimate that 1/3 of the energy should fall in the central region of intensity above the ablation threshold, the energy density in this region will be ~100 J/cm^2. If we assume that the vaporization efficiency of this laser will be similar to that of the 532 nm, 10 nsec pulse of the YAG which yielded about 0.1 μm per J/cm^2, requiring about 20 J/cm^2 for full depth scribe in a 2 micron thick film of CdTe or CIS. Thus a better solution would be to use cylindrical focussing to achieve a rectangular spot of 2.5 mm by 25 μm. Since 20 J/cm^2 are required to remove the full film thickness, the scan speed should be 100 cm/sec along the long axis of the focal spot. This is a situation clearly calling for multiple beam delivery to the workpiece!

Similar considerations for the other lasers yield the following: (1) For 2 W of power from the CWP YAG at 5 kHz, cylindrical focussing to produce a 25 μm x 500 μm spot would work well with translation at 25 cm/sec. (2) For our FLP YAG at its maximum PRF of 30 Hz, and its pulse energy of 100 mJ, the focus would have to be 25 μm x 15 cm with a translation speed of 45 cm/sec. Finally, (3) with the XeCl excimer laser at a PRF = 100 Hz, 100 mJ/pulse, and ideal focussing to a 25 μm x 15 cm line, the translation speed would need to be 150 cm/sec.

It should be noted that many lasers do not have diffraction-limited gaussian beam profiles. This is the case for our excimer laser and our flashlamp-pumped YAG. However, configurations are available using injection seeding and/or more sophisticated unstable resonator optics which should yield acceptable performance for use of an excimer laser as a scribing engine. The flashlamp-pumped YAG is probably limited by low repetition rates although a variation using diode laser pumping might remove the limitations of this system.

Scribe Quality

Obtaining the largest number of atoms removed for the fewest photons used is not the only criterion to be applied for laser scribing of PV materials. It is known that for some combinations of materials and lasers the morphology of the scribe is poor. For example we have observed cracking of the film and film delamination along the scribe edges in some situations, especially for films of Mo and ZnO on glass. In the following discussion we provide some examples of scribe morphology. Scribe profiles were studied with an optical microscope and with a stylus profilometer. We want to emphasize that these are interim results presented of a study in progress. The fact that we have observed problems in scribe morphology with a particular laser-material combination may be related to the particular focussing condition and the scan speed and may not be a fundamental property of the laser-material interaction. Especially in the cases of the CWP YAG and the copper-vapor lasers, considerable additional work remains to be done to explore beam delivery and scan speed issues.

Semiconductor Films

Figures 11-14 below provide some examples of the scribe morphology observed for two different lasers and the two semiconductor materials under study. Figs. 11 and 12 show both optical micrographs and stylus profilometer traces of scribe lines obtained with the CWP Nd:YAG laser at relatively high pulse energy density (~7.5 J/cm^2) on CdTe and CIGS. Note that this energy density is about 25 times threshold. For both semiconductors one observes a wide melt zone surrounding the scribe with "collars" protruding significantly above the plane of the film. This is clearly undesirable. Furthermore, at this energy density the center of the spot just punches through some of the Moly layer and all of the SnO_2:F layer. A very high scan speed was chosen in order to try to separate the adjacent laser spots. The optical micrograph shows that the scan speed was too slow by about a factor of two and the deepest craters occur along the line of maximum overlap. We conclude that the pulse energy is too high for clean scribing of CdTe and this study is being continued at lower pulse energy and slower scan speeds.

A similar initial study was done with the Cu-vapor laser. The results are shown in Figs. 13 and 14. For scribing

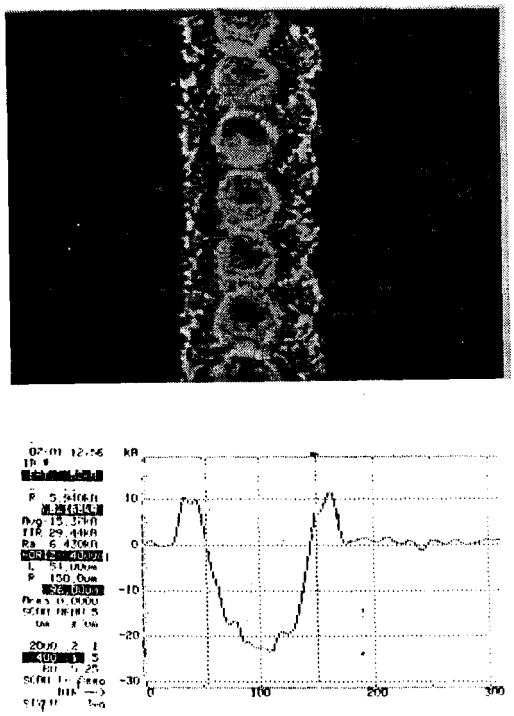

Fig. 11. Optical micrograph and stylus profilometer trace of CWP YAG scribe in CIGS at 7.5 J/cm², 5 kHz, and 25 cm/sec.

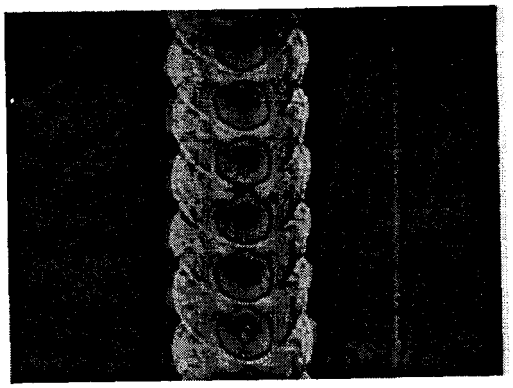

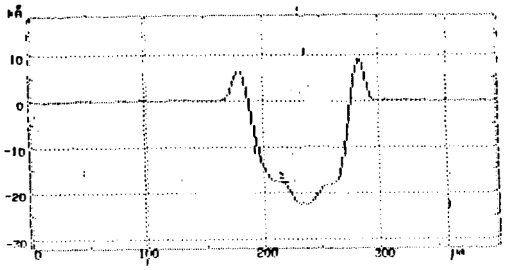

Fig. 12. Optical micrograph and stylus profilometer trace of CWP YAG scribe in CdTe at 7.5 J/cm², 5 kHz, and 25 cm/sec.

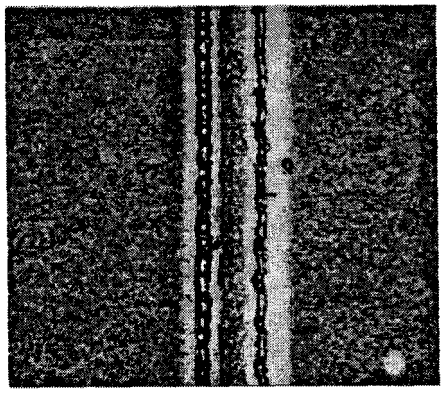

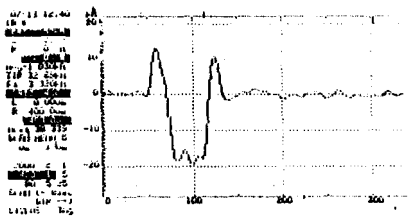

Fig. 13. Optical micrograph and stylus profilometer trace of Cu laser scribe in CIGS at 2 J/cm², 8 kHz, and 13.5 mm/sec.

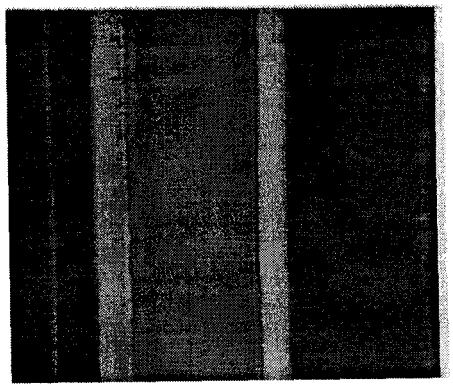

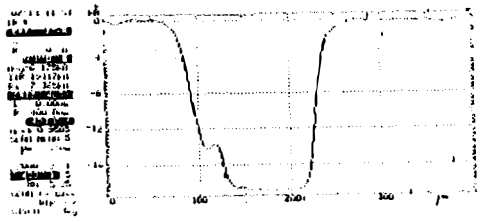

Fig. 14. Optical micrograph and stylus profilometer trace of Cu laser scribe in CdTe at 0.5 J/cm², 8 kHz, and 13.5 mm/sec.

of CIGS (Fig. 13) a narrow scribe line was achieved with a tight focus and an energy density of ~2 J/cm^2. Here the pulse duration is about 1/3 that of the CWP YAG so that the peak power density is similar. Again sharp collars are observed along the edges of the scribe which extend about 1 μm above the plane of the film. Scribing of the CdTe film was done with a softer focus (2 mm away from the best focus with the 10 cm lens). Although the scribe width in this case was about 140 μm, there is no evidence of protrudng collars around the scribe line. In this case the peak energy density was only 0.5 J/cm^2 or about twice the vaporization threshold but with about 40 overlapping pulses.

Transparent Conducting Oxides

SnO_2 has a much higher threshold than the semiconductors but readily yields clean scribes. The scribe profile obtained with the Cu-vapor laser is shown in Fig. 15. The very steep side walls are probably a consequence of the non-linear absorption for the green and yellow wavlengths of this laser in the essentially-transparent TCO. For ZnO:Al the adhesion is lower and the film tends to flake off as shown in Fig. 16 for a scribe obtained with the FLP Nd:YAG. There is slight marking of the underlying glass suggesting that the onset of absorption may be occuring at the ZnO/glass interface. By contrast, when the excimer laser is used, the scribe boundaries are very smooth with no evidence of flaking. See Fig. 17. This is consistent with the fact that the absorption is very strong at the 308 nm wavelength of the excimer.

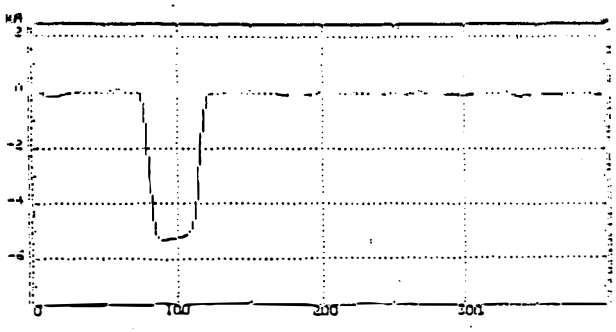

Fig. 15. Tencor profilometer trace of a Cu laser scribe in SnO_2, ~10 J/cm^2, 8 kHz, 13.5 mm/sec.

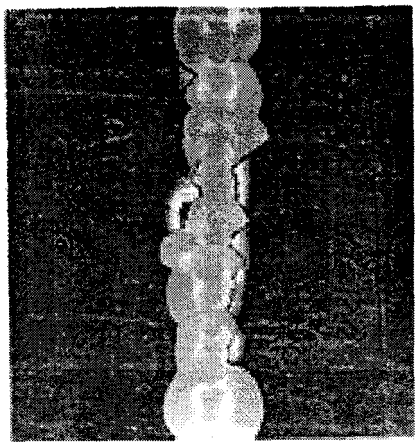

Fig. 16. Optical micrograph of FLP YAG laser in ZnO at ~15 J/cm^2, 10 Hz, 1 mm/sec.

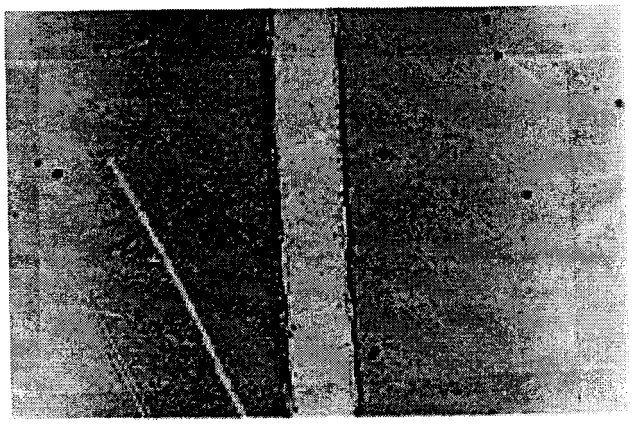

Fig. 17. Optical micrograph of excimer laser scribe in ZnO at 2.5 J/cm^2, 20 Hz, 1 mm/sec.

Molybdenum Metal

Fig. 18 shows a "scribe" of a Mo film with the Cu-vapor laser. Clearly there was too much heat load on the film which produced cracking and delamination. Further studies are planned to determine whether Moly can be scribed successfully with this laser. With the XeCl laser, a clean scribe is readily obtained for the same Moly film. This is shown in Fig. 19. The scribe morphology appears similar to that in ZnO as shown in Fig. 17 above. The similarity is presumably due to the fact that optical absorption is very high at 308 nm in both materials and the short pulse duration minimizes heat flow during the pulse.

Cylindrical Focussing

Too much energy density at the center of the focal spot can result in undesirable effects. We have seen, for example, with the flashlamp-pumped YAG at 1064 nm on CdTe films that one can get a complete scribe but there is a large heat-affected zone surrounding the scribe. When spherical lens focussing (f=10 cm) is used, the energy density at the center of the scribe line was 50 times the ablation threshold so that the weak fringes of the focal spot have enough energy density to damage a wide swath around the scribe. See Fig. 20. By contrast, the use of a 10 cm cylindrical focussing lens allows one to avoid such high energy densities at the center. With the use of a cylindrical focussing lens we have been able to achieve a clean scribe with a much smaller heat-affected zone since the peak energy density is much less. Figure 21 shows results obtained with cylindrical focussing.

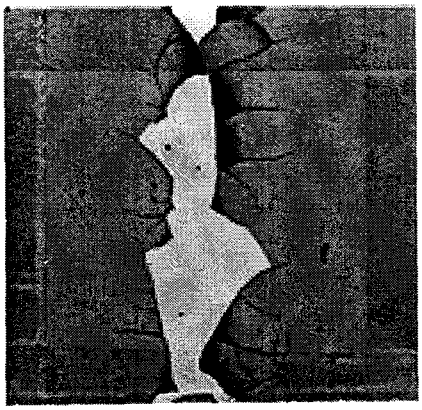

Fig. 18. Optical micrograph of Cu-laser scribe in Moly at 2.4 J/cm², 8 kHz, and 13.5 mm/sec.

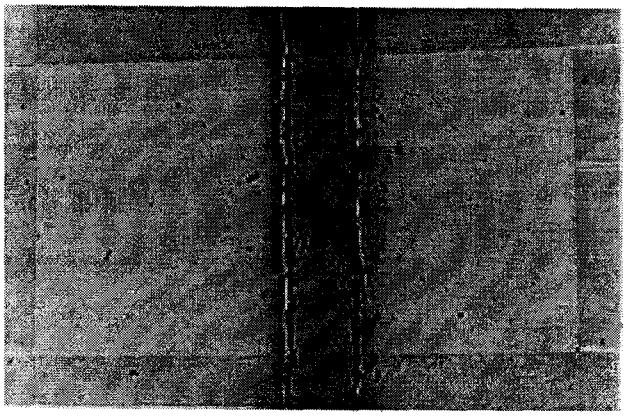

Fig. 19. Optical micrograph of excimer laser scribe in Moly at 1 J/cm², 20 Hz, and 1 mm/sec.

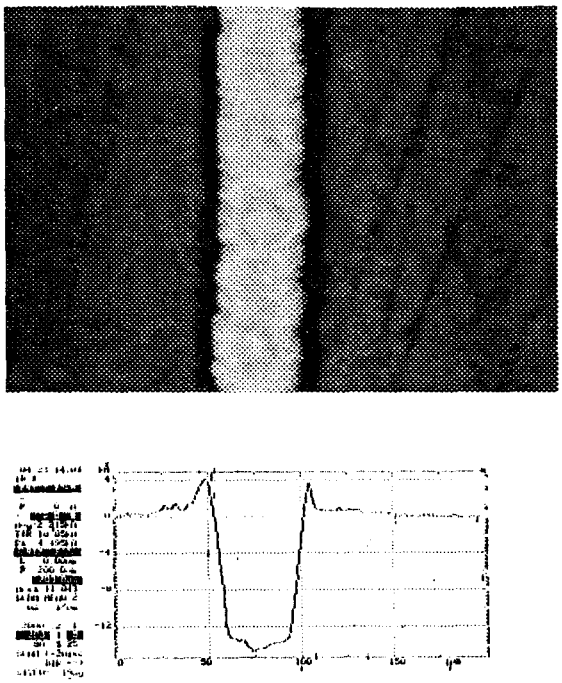

Fig. 20. Optical micrograph and stylus profilometer trace of FLP YAG scribe in CdTe with 5 J/cm² at 1064 nm, 10 Hz, 1 mm/sec, and spherical focussing.

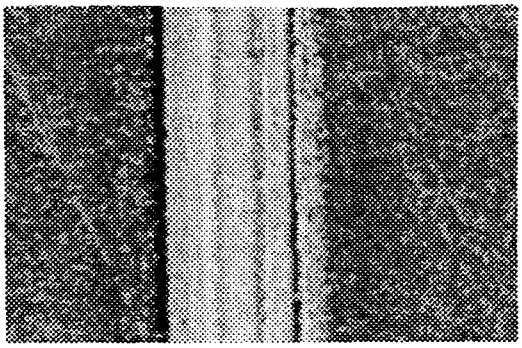

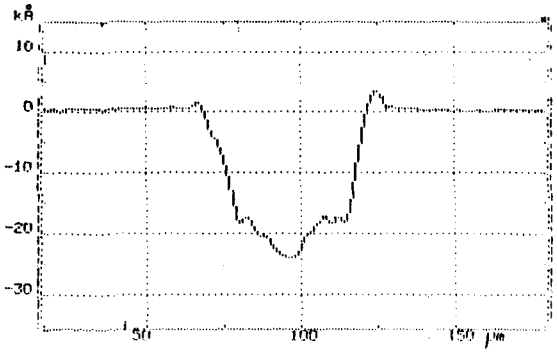

Fig. 21. Optical micrograph and stylus profilometer trace of FLP YAG laser scribe in CdTe with 3 J/cm² at 1064 nm, 10 Hz, 1.6 mm/sec, and cylindrical focussing.

Conclusions

We have determined the threshold power densities for the onset of ablation from thin films of CdTe, $CuInSe_2$, SnO_2:F, ZnO:Al, and molybdenum for four different laser systems. Optimum energy density for most efficient removal of material during scribing is strongly dependent on the wavelength of the laser and to a smaller extent on the pulse duration. The optimum energy densities range from 0.5 J/cm^2 for the 532 nm, 8 nsec YAG pulse on CdTe to 0.2 J/cm^2 for the excimer laser at 308 nm on CIS. Poor performance was seen with the 1064 nm beam on CdTe, the 532 nm beam on ZnO, and the copper laser on Mo. Excellent scribe profiles were observed with the excimer laser on Mo and ZnO. Anomalously high optimum scribe energy density values appear for 532nm on Mo. These are being remeasured.

Acknowledgments

This work was supported at UT by NREL under contract no. ZAF-5-14142-08, which has also supported the contributions of personnel and materials from Solar Cells Inc (Toledo, OH), C J Laser Corp. (Dayton, OH), and ISET (Los Angeles, CA). To SCI we are grateful for making time available to use the Nd:YAG laser and the Tencor stylus profilometer, as well as assistance with their use. C J Laser has provided the Cu vapor laser and time in their applications lab and ISET has provided the thin-film materials Mo, ZnO, and CIS.

References

[1] A. D. Compaan, "Laser Processing for Thin-Film Photovoltaics," Proc. SPIE 2403, pp. 224-231.

[2] V. Ramanathan, L.A. Russell, C.H. Liu, and P.V. Meyers, "Indoor Stability Tests on CdS/CdTe/ZnTe n-i-p Submodules," Solar Cells **28**, 129-133 (1990).

[3] J.G. O'Dowd, B.J. Johnson, R.S. Oswald, & F. Willing, "The Stability of Laser Weld Interconnects in a-Si:H Modules," Proc. 23rd IEEE PVSC-1993, pp. 926-929; F. Willing, R. Oswald, and J. Newton, "Controlling Shorts in a-Si Modules," Proc. 23rd IEEE PVSC-1993, pp. 946-949.

[4] R. Arya, "Research on Polycrystalline Thin Film Submodules Based on $CuInSe_2$ Materials," Solarex Final Technical Report. NREL contract ZN-1-19019-4 (1995).

[5] S. Nakajima, M. Abe, H. Shinohara, Y. Arai, N. Ishida, A. Satake, K. Nishi, S. Kugawa, Y. Uehara, M. Ishii, & S. Yamazaki, "High Effective Area Amorphous Silicon Solar Cell Using Excimer Laser Process," Proc. 21st IEEE PVSC-1990, 1400 .

[6] P.H. Key, D. Sands, and F.X. Wagner, "UV-Excimer Laser Ablation Patterning of II-VI Compound Semiconductors," Matls. Sci. Forum, 173-174, 59-66 (1995).

[7] L. Balazs, R. Gijbels, and A. Vertes, "Expansion of Laser-Generated Plumes Near the Plasma Ignition Threshold," Analytical Chemistry **63**, 314 (1991).

[8] R. Srinivasan & V. Mayne-Banton, Appl. Phys. Lett. 41, 576, (1982); J.E. Andrew, P.E. Dyer, D. Forster, and P.H. Key, "Direct Etching of Polymeric Materials Using a XeCl Laser," Appl. Phys. Lett. 43, 717-719 (1983).

[9] A.D. Compaan, I. Matulionis, M.J. Miller, and U.N. Jayamaha, "Optimization of Laser Scribing for Thin-Film Photovoltaics," to appear in Proc. 25th IEEE PVSC--1996 (Washington, D.C., May 13-17, 1996).

[10] L. Quercia, S. Avagliano, A. Parretta, E. Salza, and P. Menna, "Laser Patterning of $CuInSe_2$/Mo/SLS Structures for the Fabrication of CuIn Se_2 Submodules," Matls. Sci. Forum, 173-174, 53-58 (1995).

REPORT DOCUMENTATION PAGE

Form Approved
OMB NO. 0704-0188

1. AGENCY USE ONLY (Leave blank)	2. REPORT DATE	3. REPORT TYPE AND DATES COVERED
	October 1996	Annual Technical Progress Report, 12 April 1995 - 11 April 1996

4. TITLE AND SUBTITLE

Optimization of Laser Scribing for Thin-Film PV Modules; Annual Technical Progress Report, 12 April 1995 - 11 April 1996

5. FUNDING NUMBERS

C: ZAF-5-14142-08
TA: PV631101

6. AUTHOR(S)

A.D. Compaan, U. Jayamaha, I. Matulionis, and M.J. Miller

7. PERFORMING ORGANIZATION NAME(S) AND ADDRESS(ES)

University of Toledo
Toldeo, Ohio 34606

8. PERFORMING ORGANIZATION REPORT NUMBER

9. SPONSORING/MONITORING AGENCY NAME(S) AND ADDRESS(ES)

National Renewable Energy Laboratory
1617 Cole Blvd.
Golden, CO 80401-3393

10. SPONSORING/MONITORING AGENCY REPORT NUMBER

TP-451-21718

DE96013114

11. SUPPLEMENTARY NOTES

NREL Technical Monitor: B. von Roedern

12a. DISTRIBUTION/AVAILABILITY STATEMENT

12b. DISTRIBUTION CODE

UC-1263

13. ABSTRACT *(Maximum 200 words)*

This report covers the first year of a 2-year project to investigate the use of four different types of lasers for scribing materials used for polycrystalline thin-film photovoltaics. The materials under investigation include semiconductors (cadmium telluride and copper indium gallium diselenide), transparent conducting oxides (fluorine-doped tin oxide and aluminum-doped zinc oxide), and a metal (molybdenum). The laser systems are all commercially available and were chosen for the range of pulse durations and wavelengths. In collaboration with Solar Cells, Inc., International Solar Electric Technologies, and C J Lasers, Inc., we used a continuous krypton-lamp-pumped, Q-switched Nd:YAG laser; a flashlamp-pumped Nd:YAG laser; a copper-vapor laser; and a XeCl-excimer laser. The laser systems and beam focusing options are being evaluated from the pont of view of the efficiency of pulse-energy utilization, potential for high scribing velocity, and scribe quality (e.g., electrical isolation, narrow scribe width, small heat-affected zone, and minimum ejecta rim at the scribe edge).

14. SUBJECT TERMS

photovoltaic modules ; polycrystalline thin-film semiconductors ; conducting oxides ; laser scribing systems

15. NUMBER OF PAGES
20

16. PRICE CODE

17. SECURITY CLASSIFICATION OF REPORT	18. SECURITY CLASSIFICATION OF THIS PAGE	19. SECURITY CLASSIFICATION OF ABSTRACT	20. LIMITATION OF ABSTRACT
Unclassified	Unclassified	Unclassified	UL